

Figure S 1: Size distribution of the cell suspension studied, the line is a normal distribution with the same average and standard deviation than the suspension

Supporting Information

Polydispersity of the cells Thanks to the two photon microscope's images, it is possible to measure the radius of the cells, and thus to access the size distribution of the suspension. The average particle size is $7.5 \mu\text{m}$ with a standard deviation of $1.7 \mu\text{m}$. The line in Fig. S1 represents a normal distribution with the same average and standard deviation than our suspension.

Two-photon microscopy: A two-photon microscope was then used in order to take pictures of the suspension at several heights in order to have a 3D representation of the suspension, as the one showed in the movie file S1.

2D Fractal Dimension

Following the protocol of Allain and Jouhier [1], the fractal dimension of our suspension can be measured in two dimensions. Using a circle of radius R , an aggregate is isolated and the cells present in the cluster are counted. This enables us to plot Fig. S1, where the slope of the curve represents the inverse of the fractal dimension. Fig. S1 shows that for the fibrob-

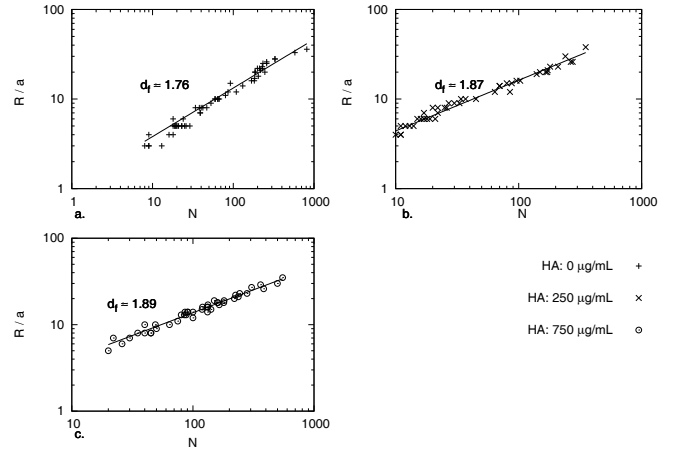


Figure S 2: Ratio of the size of an aggregate with the size of a single cell as a function of the number of cells constituting the aggregate. (A) Without HA. (B) With $250 \mu\text{g/mL}$ of HA. (C) With $750 \mu\text{g/mL}$ of HA.

last cell suspensions without HA, $df = 1.76$, which is close to 1.7. However when HA is added at either a concentration of $250 \mu\text{g/mL}$ or $750 \mu\text{g/mL}$, the fractal dimension increases to 1.87 and 1.89, respectively. These values are within the range of values (1.48 - 1.94) previously reported for two dimensional aggregation of particles under different shear and coagulant dose conditions [2]. Moreover, by using the relationship between 2D and 3D fractal dimension recently proposed by Ganguly et al. [3], we can estimate the 3D fractal dimension from our 2D fractal dimension, should range from 2.58 to 2.65, with and without the HA respectively.

Decomposition of the Master Curve

The Figure S3 shows the same mastercurve as in the article, but with the different shear rates decomposed in four graphs. Interestingly, the data for very high shear rates (900 s^{-1}) seem to deviate from the models, following a Krieger and Dougherty model with a maximum packing volume fraction of 0.7. This can be explained by the deformability of cells, which are not absolute hard spheres. Indeed, suspended NIH3T3 cells are more elastic spheres, with an elastic modulus of $100 \text{ Pa} \pm 10 \text{ Pa}$ [4]. Their deformability at high shear rates can therefore not be neglected.

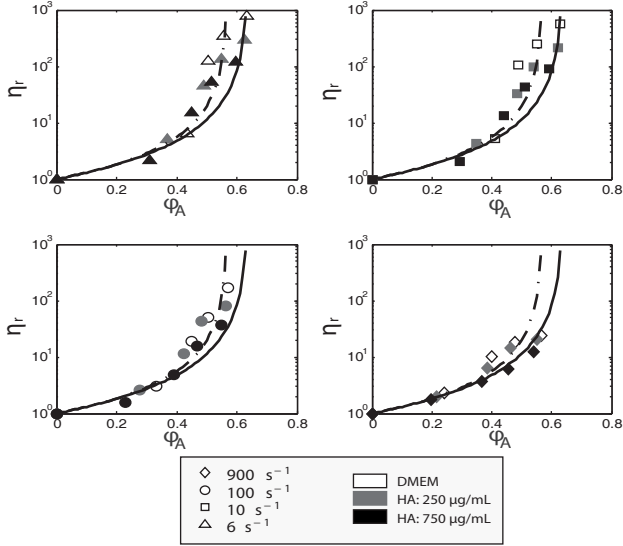


Figure S 3: Relative viscosity as a function of the effective volume fraction for different HA concentrations and for different shear rates. The solid line is the Krieger and Dougherty model with $\varphi_0 = 0.64$, the broken line is the Krieger and Dougherty model with $\varphi_0 = 0.57$.

References

- [1] C. Allain, B. Jouhier, *Simulation cinétique du phénomène d'agrégation*, J. Phys. Lettre, 45 (1983), pp. 421–428.
- [2] R.K. Chakraborti, K.H. Gardner, J.F. Atkinson, J.E. Benschoten, *Changes in fractal dimension during aggregation*, Water Research, 37 (2003), pp. 873–883.
- [3] S. Ganguly, S. Basu, S. Sikdar, *Determination of the aggregate fractal dimensions in colloidal nanofluids*, Proc IMechE Part N: J Nanoengineering and Nanosystems, 226(1) (2023).
- [4] F. Wottawah, S. Schinkinger, B. Lincoln, R. Ananthakrishnan, M. Romeyke, J. Guck, J. Kas, *Optical rheology of biological cells*, Phys. Rev. Lett., 94 (2005), pp. 098103.